GEOPHYSICS, VOL. 54, NO. 6 (JUNE 1989); P. 766–774, 8 FIGS.

Singularity removal: A refinement of resistivity modeling techniques

T. Lowry*, M. B. Allen‡, and P. N. Shive*

ABSTRACT

Modeling techniques commonly exhibit errors of 3 to 10 percent or more in the calculation of apparent resistivities over earth models for which analytic solutions are easily available. A singularity occurs in the solution of any elliptic partial differential equation for which the forcing function is not smooth. The inability to adequately represent in discrete space a discontinuous function (in this case, the delta function describing the introduction of current at a point) commonly results in numerical error near the source of a modeled singularity.

Inspection of an integrated finite-difference method for modeling the dc resistivity geophysical technique indicates much of the error encountered is of singular origin. A procedure is herein detailed by which the singularity is mathematically removed from the modeling process and reintroduced as a last step, thus preventing it from contributing to the numerical error. Using this procedure, the average error in apparent resistivity values for a model of a polar-dipole traverse over a nonconducting sphere is reduced by 40 percent. For a dipole-dipole traverse of a two-layer model the error decreases by 75 percent, and in the case of a Wenner profile of a model of a vertically faulted earth, the average error is diminished by 90 percent.

INTRODUCTION

Data acquired in electrical prospecting are most often interpreted by comparison to solutions for the electrical responses from various earth models. The geophysicist's ability to interpret such data is constrained by the variety and complexity of solutions available for comparison.

The first numerical approach to modeling resistivity and other electrical geophysical methods surfaced about 30 years ago with the introduction by Alfano (1959) of an integral equation formulation over a multilayered conductive medium. Nothing more was attempted in this vein for a full decade, however, until Dieter et al. (1969) applied the same method to computing the electrical response over various spheroidal and ellipsoidal bodies. At about the same time, Jepsen (1969) reported a finite-difference representation of the two-dimensional (2-D) resistivity problem, and Coggon (1971) presented a 2-D finite-element technique.

Integral equation solutions have been the most popular of the numerical approximations discussed in the literature (Pratt, 1972; Bakbak, 1977; Lee, 1975; Barnett, 1972; and Hohmann, 1975). More recently, the technique has found application in the modeling of various conditions which complicate the interpretation of resistivity data, such as topography overlying the targeted heterogeneity (Spiegel et al., 1980; Xu et al., 1988) and the delineation of conductive bodies using buried current electrodes (Daniels, 1977; Poirmeur and Vasseur, 1988).

Discussion of the finite-element and finite-difference methods is a bit more sparse, perhaps because the computational expense associated with these methods is large relative to the integral equation technique. The generality of a volumetric discretization can be advantageous, however, especially if the modeler wishes to incorporate such features as geologic noise, gradational change, or even anisotropy in earth parameters.

Several variations on the 2-D problem have been presented, including 2-D finite-difference simulations developed by Mufti (1976), Dey and Morrison (1979a), and Mundry (1984). Fox et al. (1980) looked at topographic effects using finite-element approximations, and Bibby (1978) proposed a finite-element scheme expressly for bodies having a vertical axis of symmetry. It was not until 1979, however, that Dey and Morrison (1979b) reported an actual three-dimensional (3-D) finite-difference algorithm. Pridmore et al. (1981) followed soon after with an investigation of a 3-D finite-element technique.

Both papers dealing with 3-D approximations acknowledged an error of from 3 to 10 percent in the calculation of apparent resistivities over earth models having analytic solu-

Manuscript received by the Editor July 29, 1988; revised manuscript received November 21, 1988.
*Department of Geology and Geophysics, University of Wyoming, P.O. Box 3006, Laramie, WY 82071.
‡Department of Mathematics, University of Wyoming, P.O. Box 3036, Laramie, WY 82071.

tions. We have determined that much of this error is due to a singularity, or discontinuity, which occurs in the forcing function of the partial differential equation describing the problem.

It should be noted that Okabe (1979) and others have discussed singularities occurring in the integral equation numerical approach. The singularities they treated, however, arise from the method itself and hence are quite different from those encountered using the finite-difference and finite-element techniques. Charbeneau and Street (1979) addressed those point singularities which occur in the finite-element modeling of groundwater flow, but no one up to this point has described a satisfactory means of handling singularities typically found in volumetric discretizations of the electrical resistivity problem.

While it is possible to mitigate singular error by using very fine grids, in three dimensions this radically increases the computational expense. In this paper, a method is employed by which the singularity is removed from the numerical process. This avoids the associated error and improves the accuracy of the solution while maintaining an affordable grid size. Several examples are given demonstrating the increased accuracy of the new method. Since the changes made require virtually no additional computation time, the numerical approximation incorporating singularity removal is a distinct improvement over previous methods.

THE DOMAIN EQUATION

The partial differential equation governing the resistivity problem is easily derived from a few basic tenets of electrical theory. Using the principle of conservation of charge and the continuity equation as it applies to charge flow, we have for a point source

$$\nabla \cdot \mathbf{J} = \frac{\partial \rho}{\partial t}\,\delta(\mathbf{x} - \mathbf{x}_s),$$

where $\mathbf{J}$ is current density and $\mathbf{x}_s$ is the spatial position of a point source at which the charge density ρ is specified. Ohm's law relates current density to the conductivity σ of the medium and the electric field $\mathbf{E}$ as

$$\mathbf{J} = \sigma\mathbf{E}.$$

If the electric field is stationary, it can be defined in terms of a scalar potential Φ as

$$\mathbf{E} = -\nabla\Phi.$$

Combining all three of the above relations yields

$$\nabla \cdot \Big[\sigma(\mathbf{x})\nabla\Phi(\mathbf{x})\Big] = -\frac{\partial \rho}{\partial t}\,\delta(\mathbf{x} - \mathbf{x}_s). \tag{1}$$

The charge source in the case of the resistivity method is an injected current, and thus

$$\frac{\partial \rho}{\partial t}\,\delta(\mathbf{x} - \mathbf{x}_s) = I\delta(\mathbf{x} - \mathbf{x}_s), \tag{2}$$

where I is the current. After substituting equation (2) into equation (1), the domain equation to be solved numerically becomes

$$\nabla \cdot \Big[\sigma(\mathbf{x})\nabla\Phi(\mathbf{x})\Big] = -I\delta(\mathbf{x} - \mathbf{x}_s). \tag{3}$$

DISCRETIZATION AND FINITE-DIFFERENCE APPROXIMATION

We use the integrated finite-difference approach to the 3-D resistivity problem introduced by Dey and Morrison (1979b) and used more recently by James (1985). The problem is discretized in such a way as to place the nodes at which potential is to be determined at the corners of conductive blocks, each block having a constant conductivity σ throughout its volume. Individual nodes are indexed in the x-direction by $i = 1, 2, 3, \cdots, L$; in the y-direction by $j = 1, 2, 3, \cdots, M$; and in the z-direction by $k = 1, 2, 3, \cdots, N$.

Conductivities are allowed to vary from block to block in some approximation of the desired spatial distribution, with the conductive blocks indexed such that $\sigma_{i,j,k}$ is the conductivity of the block lying just below, behind, and to the right of node (i, j, k) on a left-handed coordinate system with z increasing downward (see Figure 1). We make the assumption that the grid is uniform in each of the coordinate directions with grid spacings Δx, Δy, and Δz. At each node (i, j, k), equation (3) can then be integrated over the elemental volume $\Delta V = \Delta x\Delta y\Delta z$. Green's theorem is applied, converting the volume integral to a surface integral and yielding the integrated equation

$$\iint_{S_{i,j,k}} \sigma(\mathbf{x})\frac{\partial\Phi(\mathbf{x})}{\partial n}\,ds_{i,j,k} = -I\delta(x_i - x_s)\delta(y_j - y_s)\delta(z_k - z_s), \tag{4}$$

where $\partial/\partial n$ is the outward normal derivative and we assume that (x_s, y_s, z_s) coincides with a node. After substituting a first-order forward finite-difference approximation for the $\partial\Phi/\partial n$ term in equation (4) and evaluating the surface integral, the equation becomes

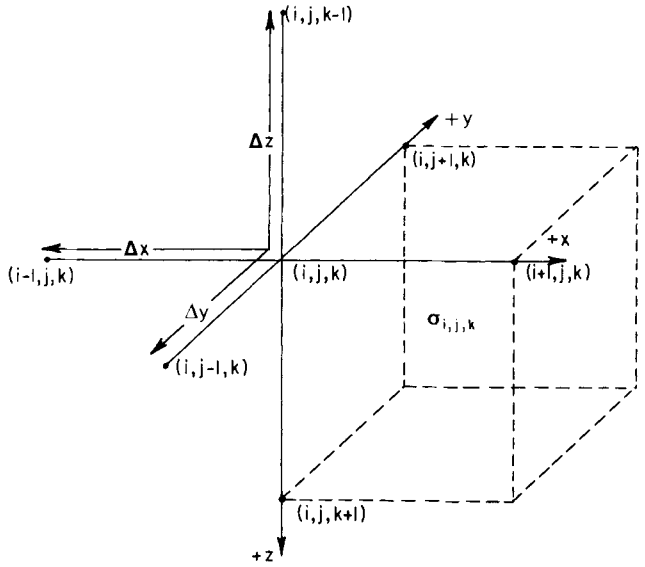

FIG. 1. Stencil depicting the indexing scheme used for the integrated finite-difference discretization (adapted from James, 1985).

$$C_{i,j,k-1}\Phi_{i,j,k-1}+C_{i,j-1,k}\Phi_{i,j-1,k}+C_{i-1,j,k}\Phi_{i-1,j,k}+C_{i,j,k}\Phi_{i,j,k}+C_{i+1,j,k}\Phi_{i+1,j,k}+C_{i,j+1,k}\Phi_{i,j+1,k}+C_{i,j,k+1}\Phi_{i,j,k+1}=-I\delta(x_i-x_s)\delta(y_j-y_s)\delta(z_k-z_s), \quad (5)$$

in which the coupling coefficients C are defined as

$$C_{i,j,k-1}\equiv\frac{\Delta x\Delta y}{4\Delta z}\left[\sigma_{i-1,j-1,k-1}+\sigma_{i,j-1,k-1}+\sigma_{i-1,j,k-1}+\sigma_{i,j,k-1}\right], \quad (5a)$$

$$C_{i,j-1,k}\equiv\frac{\Delta x\Delta z}{4\Delta y}\left[\sigma_{i-1,j-1,k-1}+\sigma_{i,j-1,k-1}+\sigma_{i-1,j-1,k}+\sigma_{i,j-1,k}\right], \quad (5b)$$

$$C_{i-1,j,k}\equiv\frac{\Delta y\Delta z}{4\Delta x}\left[\sigma_{i-1,j-1,k-1}+\sigma_{i-1,j,k-1}+\sigma_{i-1,j-1,k}+\sigma_{i-1,j,k}\right], \quad (5c)$$

$$C_{i+1,j,k}\equiv\frac{\Delta y\Delta z}{4\Delta x}\left[\sigma_{i,j-1,k-1}+\sigma_{i,j,k-1}+\sigma_{i,j-1,k}+\sigma_{i,j,k}\right], \quad (5d)$$

$$C_{i,j+1,k}\equiv\frac{\Delta x\Delta z}{4\Delta y}\left[\sigma_{i-1,j,k-1}+\sigma_{i,j,k-1}+\sigma_{i-1,j,k}+\sigma_{i,j,k}\right], \quad (5e)$$

$$C_{i,j,k+1}\equiv\frac{\Delta x\Delta y}{4\Delta z}\left[\sigma_{i-1,j-1,k}+\sigma_{i,j-1,k}+\sigma_{i-1,j,k}+\sigma_{i,j,k}\right], \quad (5f)$$

and

$$C_{i,j,k}\equiv-\left[C_{i,j,k-1}+C_{i,j-1,k}+C_{i-1,j,k}+C_{i+1,j,k}+C_{i,j+1,k}+C_{i,j,k+1}\right]. \quad (5g)$$

We solve equation (5) for the potential Φ at each of the nodes (i, j, k).

BOUNDARY CONDITIONS

For a given discretization, the problem is solvable provided the following elemental boundary conditions are met: (1) the potential Φ must be continuous across boundaries dividing elements of differing conductivities and (2) the normal component of current ($J_n \equiv \sigma\partial\Phi/\partial n$) must also be continuous at such boundaries.

Because equation (5) can be made to satisfy these conditions, we can guarantee the existence of a unique solution by imposing domain boundary conditions of the form

$$\alpha(\mathbf{x})\Phi+\beta(\mathbf{x})\frac{\partial\Phi}{\partial n}=g(\mathbf{x}) \quad (6)$$

provided $\alpha(\mathbf{x})\geq 0$; $\beta(\mathbf{x})\geq 0$; $[\alpha(\mathbf{x})+\beta(\mathbf{x})]>0$; and $\alpha(\mathbf{x})\neq 0$ for at least one boundary point $\mathbf{x}$.

Air is virtually nonconductive, so a "no-flow" Neumann condition ($\partial\Phi/\partial n=0$) is adopted at the air-earth interface $z=0$. On the other domain boundaries, however, different authors have used a variety of approximations in an attempt to find one giving the best approximation to the solution for the semiinfinite domain $z>0$. Coggon (1971) imposes both a Dirichlet condition ($\Phi=0$) and a no-flow Neumann condition on his finite-element model and then averages the results. James (1985) employs a mixed-boundary condition in which α and β in equation (6) are independent of position $\mathbf{x}$ and are, in fact, chosen to be the optimal values for a given grid extent.

Dey and Morrison (1979b) propose another mixed-boundary condition based on the physical behavior of the potential at a given distance r from a point source. The solution for a current source placed at the surface of a uniformly conductive half-space is

$$\Phi(\mathbf{x})=\frac{I}{2\pi\sigma r}, \quad (7)$$

and thus

$$\frac{\partial\Phi(\mathbf{x})}{\partial n}=-\frac{I}{2\pi\sigma r^2}\hat{\mathbf{r}}\cdot\hat{\mathbf{n}}=-\frac{\Phi(\mathbf{x})}{r}\cos\theta,$$

where θ is the angle between the unit outward normal $\hat{\mathbf{n}}$ and the radial vector $\hat{\mathbf{r}}$. Thus, equation (6) becomes

$$\frac{\cos\theta}{r}\Phi(\mathbf{x})+\frac{\partial\Phi(\mathbf{x})}{\partial n}=0. \quad (8)$$

In the event that a source-sink or dipolar current source is used at the surface, the closed-form solution over a uniform half-space is given by

$$\Phi(\mathbf{x})=\frac{I}{2\pi\sigma}\left(\frac{1}{r_a}-\frac{1}{r_b}\right), \quad (9)$$

in which r_a is the distance to the positive electrode and r_b is the distance to the negative. In this case,

$$\frac{\partial\Phi(\mathbf{x})}{\partial n}=-\frac{I}{2\pi\sigma}\left(\frac{\cos\theta_a}{r_a^2}-\frac{\cos\theta_b}{r_b^2}\right)=-\frac{I}{2\pi\sigma}\left[\left(\frac{1}{r_a}-\frac{1}{r_b}\right)\left(\frac{\cos\theta_a}{r_a}+\frac{\cos\theta_b}{r_b}\right)+\frac{\cos\theta_a-\cos\theta_b}{r_a r_b}\right],$$

yielding the mixed-boundary condition

$$\left(\frac{\cos\theta_a}{r_a}+\frac{\cos\theta_b}{r_b}\right)\Phi(\mathbf{x})+\frac{\partial\Phi(\mathbf{x})}{\partial n}=-\frac{I}{2\pi\sigma}\left(\frac{\cos\theta_a-\cos\theta_b}{r_a r_b}\right). \quad (10)$$

If the conductivity were not homogeneous, equations (8) and (10) would each contain additional terms reflecting the perturbation of the potential due to the heterogeneity. The effects of the perturbation decay with distance, however, making the two boundary conditions acceptable approximations given that the boundary is in some sense far away

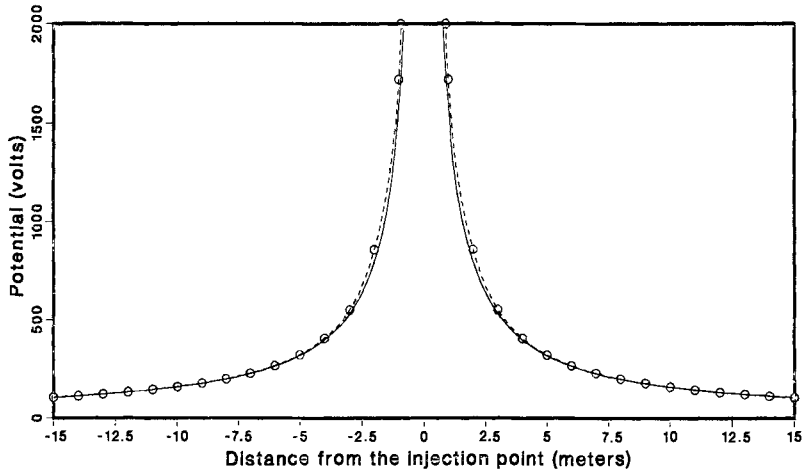

FIG. 2. Analytic (solid line) and numerical (broken) solutions for the potential about a 100 A current injection point over a half-space of constant conductivity .01 S/m.

from those parts of the domain at which the solution is of interest. We opted to incorporate equations (8) and (10) as the boundary conditions on our model simply because they seemed the most physically reasonable of those considered. Dey and Morrison (1979b) also proposed that grid cells be lengthened near the computational boundaries of the domain in an effort to reduce the error associated with the approximate nature of the boundary conditions. This device is useful only if one can balance the tradeoff between diminishing effects of boundary error and the poor approximation that results from using elongated grid blocks (Pridmore et al., 1981). Having no rigorous means by which to determine such a balance, we chose to use uniform grids throughout.

SINGULARITY REMOVAL

A singularity arises in the solution of a given elliptic partial differential equation

$$\nabla \cdot (\sigma \nabla \Phi) = f(\mathbf{x})$$

whenever the right-hand side function $f(\mathbf{x})$ is not smooth (Fox, 1979). Certainly the delta function describing the right-hand side of equation (3) is not smooth, and so we expect to see a singularity in Φ centered at any point source or source sink of charge.

Straightforward numerical approximations typically give poor results near such singularities, and indeed, for the potential over a homogeneous conductivity distribution, comparison of the integrated finite-difference numerical solution to that calculated using relation (7) indicates a systematic error in the model solution. Figure 2 is a plot of the two curves. Because the potential gradient is so high near the charge source, the two curves appear to be very close. However, when we look at the percent error of the numerical solution, we find the error is actually relatively large near the current injection point. Figure 3 illustrates the percent error in potential over a uniform half-space in the presence of a singularity with data points represented as open circles indicating the error due to a single point source of current and open squares delineating the error associated with a source directly adjacent to a current sink.

Fox (1979) discusses two relatively simple techniques commonly used to treat singular error. Grid refinement near the singular point decreases the error by rapidly reducing the size of the higher order terms in the truncation error of the difference scheme. However, the coding difficulties which must be overcome in order to permit the arbitrary location of a point source make the grid-refinement approach unwieldy.

The second, and preferred, method for removing singular error exploits the linearity of the problem by splitting the potential in equation (3) into two parts:

$$\Phi(\mathbf{x}) = \Phi_r(\mathbf{x}) + \Phi_s(\mathbf{x}). \tag{11}$$

Here Φ_s represents the response to the singularity, and Φ_r represents the regular or nonsingular part of the potential.

An average conductivity $\bar{\sigma}$ for the domain Ω can be defined as

$$\bar{\sigma} = \int_\Omega \sigma(\mathbf{x})\, d\mathbf{x} \Big/ \int_\Omega d\mathbf{x} = \sum_{i,j,k=1}^{L,M,N} \sigma_{i,j,k}/LMN.$$

Then for a point source located at the surface, Φ_s is the analytic or closed-form solution to the partial differential equation

$$\bar{\sigma}\nabla^2\Phi_s = -I\delta(\mathbf{x} - \mathbf{x}_s) \tag{12}$$

given by

$$\Phi_s = \frac{I}{2\pi\bar{\sigma}r}, \tag{13}$$

where r is the distance from the singularity. Virtually all of the singular error in the numerical model is contained in the singular part of the potential, so the sleight of hand we perform here is to treat Φ_s as a known quantity given by equation (13), substitute equation (11) into the domain equation (3), and then subtract the singular part of the equation as represented in equation (12). This leaves

$$\nabla \cdot \left\{ \sigma(\mathbf{x})\nabla\Phi_r(\mathbf{x}) + [\sigma(\mathbf{x}) - \bar{\sigma}]\nabla\Phi_s(\mathbf{x}) \right\} = 0.$$

Moving the known part of the relation to the right-hand side,

the domain equation, which is used to numerically solve for the unknown Φ_r, becomes

$$\nabla \cdot [\sigma(\mathbf{x})\nabla\Phi_r(\mathbf{x})] = -\nabla \cdot \left\{[\sigma(\mathbf{x}) - \sigma]\nabla\Phi_s(\mathbf{x})\right\}. \quad (14)$$

Applying the same discretization scheme as was described earlier, integrating about each node point, and substituting the forward finite-difference approximation for the derivative terms yields

$$\begin{aligned}
&C_{i,j,k-1}\Phi^r_{i,j,k-1} + C_{i,j-1,k}\Phi^r_{i,j-1,k} + C_{i-1,j,k}\Phi^r_{i-1,j,k} \\
&\quad + C_{i,j,k}\Phi^r_{i,j,k} + C_{i+1,j,k}\Phi^r_{i+1,j,k} \\
&\quad + C_{i,j+1,k}\Phi^r_{i,j+1,k} + C_{i,j,k+1}\Phi^r_{i,j,k+1} \\
&= \left(\bar{\sigma}\frac{\Delta x\Delta y}{\Delta z} - C_{i,j,k-1}\right)\Phi^s_{i,j,k-1} \\
&\quad + \left(\bar{\sigma}\frac{\Delta x\Delta z}{\Delta y} - C_{i,j-1,k}\right)\Phi^s_{i,j-1,k} \\
&\quad + \left(\bar{\sigma}\frac{\Delta y\Delta z}{\Delta x} - C_{i-1,j,k}\right)\Phi^s_{i-1,j,k} \\
&\quad + \left[-2\bar{\sigma}\left(\frac{\Delta x\Delta y}{\Delta z} + \frac{\Delta x\Delta z}{\Delta y} + \frac{\Delta y\Delta z}{\Delta x}\right) - C_{i,j,k}\right]\Phi^s_{i,j,k} \\
&\quad + \left(\bar{\sigma}\frac{\Delta y\Delta z}{\Delta x} - C_{i+1,j,k}\right)\Phi^s_{i+1,j,k} \\
&\quad + \left(\bar{\sigma}\frac{\Delta x\Delta z}{\Delta y} - C_{i,j+1,k}\right)\Phi^s_{i,j+1,k} \\
&\quad + \left(\bar{\sigma}\frac{\Delta x\Delta y}{\Delta z} - C_{i,j,k+1}\right)\Phi^s_{i,j,k+1}. \quad (15)
\end{aligned}$$

The coupling coefficients C are identical to those defined for equation (5).

For the case of a single charge source, the boundary conditions on the problem do not change with the splitting of the potential into its component parts. At the ground surface, we now have

$$\frac{\partial}{\partial n}\left[\Phi_r(\mathbf{x}) + \Phi_s(\mathbf{x})\right] = 0,$$

yielding

$$\frac{\partial\Phi_r(\mathbf{x})}{\partial n} = -\frac{\partial\Phi_s(\mathbf{x})}{\partial n} = 0, \quad (16)$$

which is the no-flow Neumann condition we had before. Over the other boundaries, the mixed condition we had previously becomes

$$\frac{\cos\theta}{r}\left[\Phi_r(\mathbf{x}) + \Phi_s(\mathbf{x})\right] + \frac{\partial}{\partial n}\left[\Phi_r(\mathbf{x}) + \Phi_s(\mathbf{x})\right] = 0,$$

which, when known parts are placed on the right-hand side, gives

$$\frac{\cos\theta}{r}\Phi_r(\mathbf{x}) + \frac{\partial\Phi_r(\mathbf{x})}{\partial n} = -\left[\frac{\cos\theta}{r}\Phi_s(\mathbf{x}) + \frac{\partial\Phi_s(\mathbf{x})}{\partial n}\right] = 0; \quad (17)$$

so again the boundary condition for the regular portion is the same as that for the entire potential.

The boundary conditions are altered slightly, however, in the event that a dipolar charge source is used. Equation (10), expressed in terms of component potentials, becomes

$$\begin{aligned}
&\left(\frac{\cos\theta_a}{r_a} + \frac{\cos\theta_b}{r_b}\right)\left[\Phi_r(\mathbf{x}) + \Phi_s(\mathbf{x})\right] + \frac{\partial}{\partial n}\left[\Phi_r(\mathbf{x}) + \Phi_s(\mathbf{x})\right] \\
&\quad = -\frac{I}{2\pi\sigma}\left(\frac{\cos\theta_a - \cos\theta_b}{r_a r_b}\right).
\end{aligned}$$

Rearranging terms and recalling that Φ_s is an exact solution to a semiinfinite domain problem with uniform conductivity, we find

$$\begin{aligned}
&\left(\frac{\cos\theta_a}{r_a} + \frac{\cos\theta_b}{r_b}\right)\Phi_r(\mathbf{x}) + \frac{\partial\Phi_r(\mathbf{x})}{\partial n} \\
&\quad = -\left(\frac{\cos\theta_a}{r_a} + \frac{\cos\theta_b}{r_b}\right)\Phi_s(\mathbf{x}) - \frac{\partial\Phi_s(\mathbf{x})}{\partial n} \\
&\quad\quad - \frac{I}{2\pi\sigma}\left(\frac{\cos\theta_a - \cos\theta_b}{r_a r_b}\right) = 0. \quad (18)
\end{aligned}$$

Thus, the forcing function on the boundary condition is made to disappear.

It is worth noting that although the straightforward application of the integrated finite-difference method gives a poor representation around singularities, the solution does converge with refinement of the grid mesh. Figure 4 is a plot illustrating the convergence over a uniformly conductive half-space of the scheme without singularity removal and with singularity removal incorporated. The log-log convergence plot is designed to test the hypothesis that the error is proportional to Δ^n for some power n, where Δ is the largest of the grid-mesh dimensions Δx, Δy, and Δz. The plot without singularity removal suggests $n \simeq 2$, which is in agreement with standard theory regarding elliptic equations as approximated by a seven-point finite-difference method (Birkhoff and Lynch, 1984). Note that once the singularity has been eliminated, allowing the numerical scheme to model only the smooth part of the solution, the magnitude of the error is typically much smaller. In fact, for

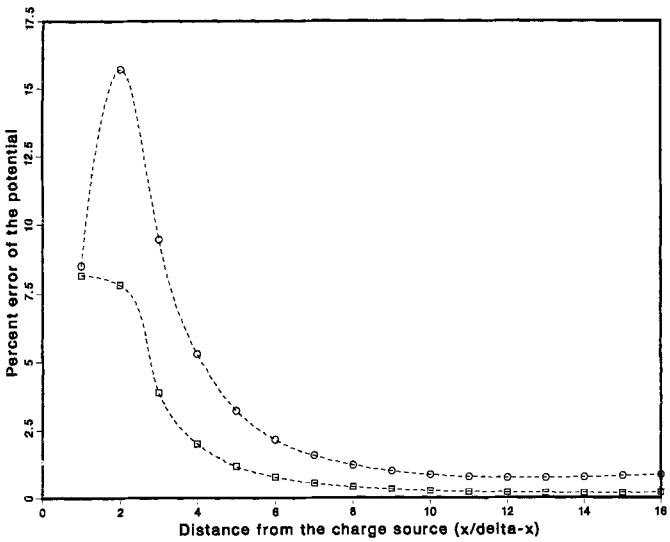

FIG. 3. Percent error of the numerical solution for potential near singularities due to a point source (denoted by open circles) and source sink (squares).

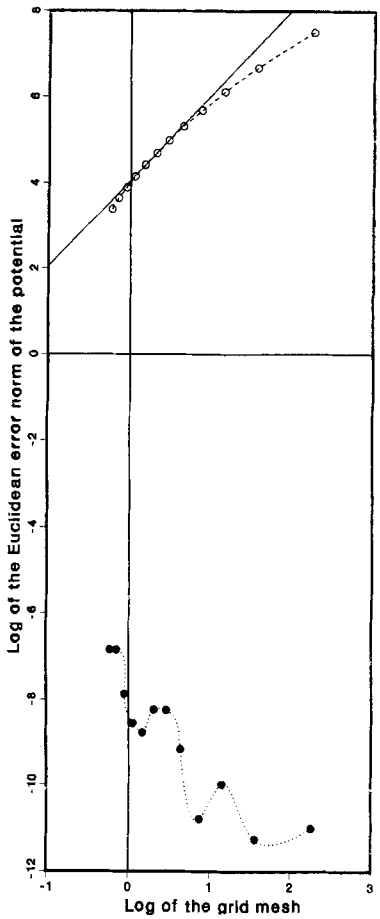

FIG. 4. Log of the Euclidean error norm of the potential versus log of the grid mesh for a uniform half-space. Results without singularity removal are represented as a dashed line; those with singular error removed are dotted. The unbroken line, having slope 2, shows the favorable comparison between actual and expected convergence with refinement of the grid.

the uniformly conductive case the error associated with the smooth part vanishes as well: the small, erratic errors traced by the dotted curve in Figure 4 are comparable in magnitude to the errors inherent in the algebraic solution of the matrix equation which results from the discretization of the problem.

MATRIX FORMULATION

The discretized equation (15) in conjunction with the boundary conditions (16), (17), and (18) is evaluated at each of the nodes (i, j, k) and the resulting system of equations is then assembled in a matrix form which can be expressed in matrix notation as

$$\mathbf{C}\Phi_r = \mathbf{s}.$$

Here $\mathbf{C}$ is a septadiagonal, diagonally dominant symmetric matrix of dimension $LMN \times LMN$ containing the coupling coefficients and is dependent only on the geometry and physical property distribution of the grid (Dey and Morrison, 1979b); Φ_r is the solution vector containing the unknown values of the regular part of the potential; and $\mathbf{s}$ holds the forcing terms which resulted from subtraction of the singularity.

The system of equations was solved using a conjugate gradient algorithm found in Obeysekare et al. (1987) with a simple incomplete L-U decomposition preconditioner.

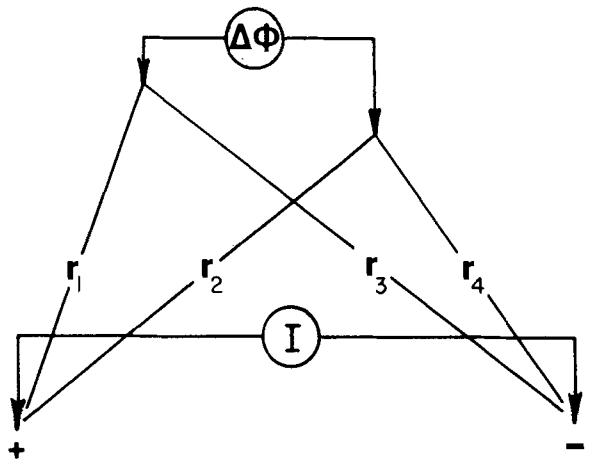

FIG. 5. An arbitrary dc resistivity electrode array.

CALCULATION OF APPARENT RESISTIVITY VALUES

As suggested by equation (11), to get the actual potentials at the nodes (i, j, k), we must add the numerically determined values Φ_r to the singularity response embodied in Φ_s. Once this is accomplished, the apparent resistivity for any arbitrary arrangement of current and potential electrodes at the ground surface is given by

$$\rho_a = \frac{2\pi\Delta\Phi}{I}\left(\frac{1}{1/r_1 - 1/r_2 - 1/r_3 + 1/r_4}\right),$$

where the distances r are as illustrated in Figure 5.

Over a homogeneous half-space, the apparent resistivity ρ_a would represent the true resistivity of the medium. In the case of a heterogeneous distribution of conductivity, ρ_a is the true resistivity value that would be necessary if the conductivity were in fact uniform to produce the observed voltage given the electrode geometry and current used. The apparent resistivity values, once plotted and compared to type curves computed by various means over known conductivity distributions, are used to interpret data generated using the resistivity method.

COMPUTATIONAL RESULTS

Apparent resistivities are calculated over three different earth models using three different electrode arrays, chosen because they are employed fairly commonly in the field. For each model the results are plotted alongside the analytic solution, represented as an unbroken line. The numerical solution for which the singularity was not removed is represented by a dashed line and that with the singular error deleted is shown as a dotted line. The average percent error of a given apparent resistivity profile is calculated as being the sum of the percent error at each of the profile points divided by the number of points.

The first simulation is of a two-layered earth model (see Figure 6) identical to that presented as an example by Dey and Morrison (1979b, Figure 4). The systematic error in the method for which the singularity was not removed is obvious

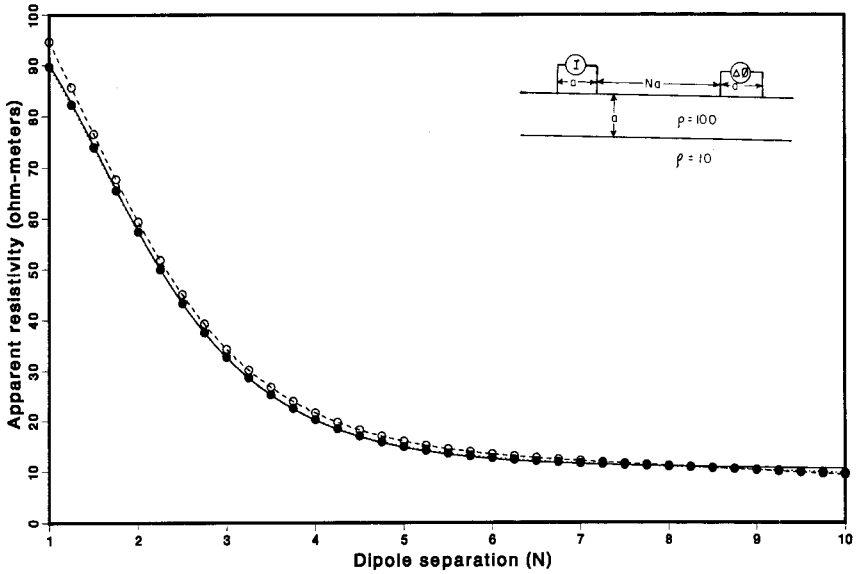

FIG. 6. Analytical and numerical results simulating a dipole-dipole array over a two-layered conductivity distribution.

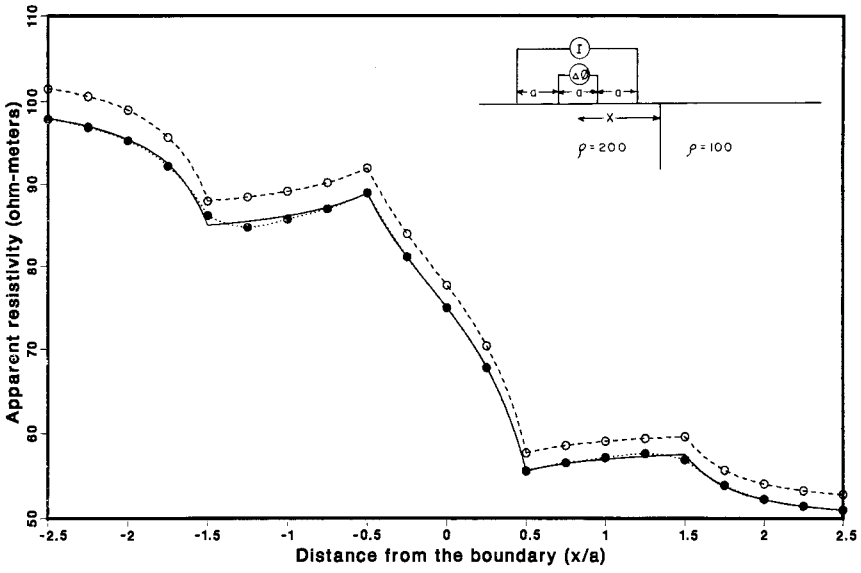

FIG. 7. Results for the Wenner array profiling a vertical discontinuity in conductivity.

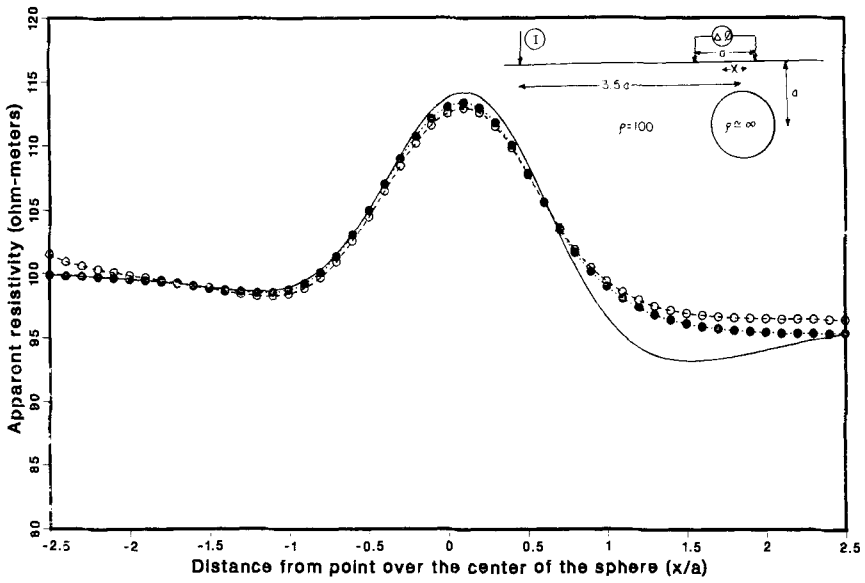

FIG. 8. Analytical versus numerical results using a pole-dipole array over a nonconducting sphere.

near the current dipole, whereas with the singularity removed the numerical curve is almost indistinguishable from the analytic solution except near the boundaries of the grid. Here boundary condition errors begin to affect both profile curves. The average error in apparent resistivity was reduced from 5.51 percent for the model without singularity removal to 1.51 percent for the model using the singularity removal technique.

The second model has a vertical discontinuity between two media of different conductivities (Figure 7), akin to a vertical fault extending to the surface. This time a Wenner array in profiling mode is used, incorporating an a spacing of 4Δ. Not surprisingly, there is a marked difference between the solutions with and without the singular error removed. The average error without singularity removal is 3.58 percent; with the singular error removed, it dropped to 0.29 percent.

The last of the models given here (Figure 8) approximates the use of a polar-dipole array with stationary current electrode, profiling over a nonconductive sphere. The improvement is much less dramatic than it was for the other two models, going from 1.37 percent average error in the apparent resistivities to 0.83 percent when the singularities were removed.

DISCUSSION

While it is apparent that the solutions calculated with the singularity removed are more accurate, it might seem from the examples given that the amount of improvement is inconsistent from one model to the next. The differences can be attributed heuristically to the nature of the electrode array used in each case. Inspection of Figure 3 suggests two properties of singular error: (1) the error falls off with increasing distance from the source of the singularity, and (2) the more singularities present, the larger the error. Thus the sphere problem shows the least improvement of the three because the polar-dipole traversing technique we used incorporates a single stationary current source and most of the measurement points are relatively distant from it. Indeed most of the error in this particular model is a result of the fact that the "nonconductive" sphere must actually be given a very small conductivity to guarantee convergence of the numerical scheme. The dipole-dipole traverse employed for the two-layer earth model again has most of the measurement points relatively distant from the current electrodes, but the improvement exhibited is somewhat greater because these are two sources of singularity instead of one. The vertical-fault model profits the most from the inclusion of the singularity removal scheme, because the Wenner array used not only involves two current sources but also requires that the measurement points be relatively nearby.

The integrated finite-difference modeling program with singularity removal requires no additional computational time to run, and thus is decidedly advantageous to use. Note that singular error is not limited to the finite-difference method; nor is it to be found solely in association with resistivity modeling. Any time one attempts to model numerically a partial differential equation containing point sources and sinks, singular error occurs. So long as there is some closed-form solution to the problem, however, subtraction of the singularity as detailed here can be used to remove the error.

CONCLUSIONS

We have proposed a 3-D integrated finite-difference scheme using a singularity removal technique for electrical resistivity modeling. Results are compared for models with and without singularity removal over conductivity distributions having analytic solutions. A marked increase in accuracy is demonstrated when the singular error is removed. The improvement is particularly dramatic for the modeling of profiling arrays such as the Wenner array, which necessitate the placement of potential electrodes relatively near the current electrodes. By employing the singularity removal scheme detailed here, an acceptable degree of accuracy can be achieved modeling any of the various electrode arrays without having to resort to an extremely fine grid mesh.

REFERENCES

Alfano, L., 1959, Introduction to the interpretation of resistivity measurements for complicated structural conditions: Geophys. Prosp., **7**, 311–366.

Bakbak, M. R., 1977, Three-dimensional numerical modeling in resistivity prospecting: Ph.D. thesis, Univ. of California, Berkeley.

Barnett, C. T., 1972, Theoretical modeling of induced polarization effects due to arbitrarily shaped bodies: Ph.D. thesis, Colorado School of Mines.

Bibby, H. M., 1978, Direct current resistivity modeling for axially symmetric bodies using the finite-element method: Geophysics, **43**, 550–562.

Birkhoff, G., and Lynch, R. E., 1984, Numerical solution of elliptic problems: Soc. Ind. Appl. Math.

Charbeneau, R. J., and Street, R. L., 1979, Modeling groundwater flow fields containing point singularities: a technique for singularity removal: Water Resources Res., **15**, 583–599.

Coggon, J. H., 1971, Electromagnetic and electrical modeling by the finite element method: Geophysics, **36**, 132–155.

Daniels, J. J., 1977, Three-dimensional resistivity and induced polarization modeling using buried electrodes: Geophysics, **42**, 1006–1019.

Dey, A., and Morrison, H. F., 1979a, Resistivity modeling for arbitrarily shaped two-dimensional structures: Geophys. Prosp., **27**, 106–136.

——— 1979b, Resistivity modeling for arbitrarily shaped three-dimensional structures: Geophysics, **44**, 753–780.

Dieter, K., Paterson, N. R., and Grant, F. S., 1969, IP and resistivity type curves for three-dimensional bodies: Geophysics, **34**, 615–632.

Fox, L., 1979, Finite differences and singularities in elliptic problems: A survey of numerical methods for partial differential equations: Oxford Univ. Press, 43–68.

Fox, R. C., Hohmann, G. W., Killpack, T. J., and Rijo, L., 1980, Topographic effects in resistivity and induced-polarization surveys: Geophysics, **45**, 75–93.

Hohmann, G. W., 1975, Three-dimensional induced polarization and electromagnetic modeling: Geophysics, **40**, 309–324.

James, B. A., 1985, Efficient microcomputer-based finite-difference resistivity modeling via Polozhii decomposition: Geophysics, **50**, 443–465.

Jepsen, A. F., 1969, Numerical modeling in resistivity prospecting: Ph.D. thesis, Univ. of California, Berkeley.

Lee, T., 1975, An integral equation and its solution for some two- and three-dimensional problems in resistivity and induced polarization: Geophys. J. Roy. Astr. Soc., **42**, 81–95.

Mufti, I. R., 1976, Finite-difference resistivity modeling for arbitrarily shaped two-dimensional structures: Geophysics, **41**, 62–78.

Mundry, E., 1984, Geoelectrical model calculations for two-dimensional resistivity distributions: Geophys. Prosp., **32**, 124–131.

Obeysekare, U., Allen, M. B., Ewing, R. E., and George, J. H., 1987, Application of conjugate gradient-like methods to a hyperbolic problem in porous media flow: Internal. J. Numer. Meth. Fluids, **7**, 551–566.

Okabe, M., 1979, Treatment of singularities in the integral equation approach: Geophysics, **44**, 2004–2006.

Poirmeur, C., and Vasseur, G., 1988, Three-dimensional modeling of a hole-to-hole electrical method: Application to the interpretation of a field survey: Geophysics, **53**, 402–414.

Pratt, D. A., 1972, The surface integral approach to the solution of the 3-D resistivity problem: Bull., Austral. Soc. Expl. Geophys., **3**, 30–50.

Pridmore, D. F., Hohmann, G. W., Ward, S. H., and Sill, W. R., 1981, An investigation of finite-element modeling for electrical and electromagnetic data in three dimensions: Geophysics, **46**, 1009–1024.

Spiegel, R. J., Sturdivant, V. R., and Owen, T. E., 1980, Modeling resistivity anomalies from localized voids under irregular terrain: Geophysics, **45**, 1164–1183.

Xu, S., Gao, Z., and Zhao, S., 1988, An integral formulation for three-dimensional terrain modeling for resistivity surveys: Geophysics, **53**, 546–552.